Pressure Drop in the Transitional Flow Regime of Annuli Associated with Mixed Convection

Ndenguma D.D., Dirker J.* and Meyer J.P.
*Author for correspondence
Department of Mechanical and Aeronautical Engineering,
University of Pretoria,
Pretoria, 0002,
South Africa,
E-mail: jaco.dirker@up.ac.za

ABSTRACT

In this experimental study, the Reynolds number limits of the transitional flow regime and friction factor characteristics were determined in the transitional flow regime of annuli. Isothermal and diabatic tests were conducted using four horizontal concentric annular passages with hydraulic diameters of 26.2, 23, 20.2 and 17 mm and respective diameter ratios of 0.327, 0.409, 0.386 and 0.483. The water in the annular passage was either heated or cooled at non-uniform temperature on the inner wall while the outer wall was insulated. The flow was both hydrodynamic and thermally developing, and the transitional flow was associated with mixed convection. The geometric size of the annular passage had a significant influence on the friction factors and Reynolds number span of the transitional flow regime. The annular geometric parameter that represent the geometric size of the annular passage was proposed and found to describe the friction factors well. Subsequently, correlations for predicting the friction factors in the transitional flow regime were developed.

INTRODUCTION

In some thermal engineering processes, flows in annular passages are commonly applied, for example, where tube-in-heat exchanger are used. Heat exchangers of different sizes are utilized depending on the heat transfer requirements and other considerations. The size of heat exchanger impacts on heat transfer coefficient and friction factor. This is evident in several calculations that are used to determine these parameters [1].

Pressure drop is important for convection heat transfer because it is associated with pumping power. Pressure drop and heat transfer coefficients are comparatively low in the laminar flow regime than in the turbulent. In many cases, the best compromise between a high heat transfer coefficient and relative low pressure drop is in the transitional flow regime. Although turbulent flow is the most preferred operating regime, however, heat exchangers may end up being operated in the transitional flow regime due to several reasons [2].

Significant amount of research have been conducted on annular flow passages, especially in the turbulent flow regime. The most notable is the research contribution by Gnielinski [3]. Van Zyl *et al.* [4] and Prinsloo *et al.* [5] investigated the effect of the heat transfer direction (from the inner wall to the annular fluid and vice versa) on the pressure drop in the turbulent flow regime of annuli of horizontal tubes. Friction factors were relatively high for the cooled annulus case. This phenomenon was attributed to temperature differences between the inner wall and the annular fluid for the heated and cooled cases.

Even though there is significant work available in the literature for annular flow in the turbulent flow regime, relatively little work is dedicated to the transitional flow regime. For circular tubes, it is generally accepted that in the transitional flow regime Reynolds numbers fall between 2 300 and 10 000 [6]. However, clear indications of where the transitional flow regime exist in annular flow passages are not yet clearly defined.

NOMENCLATURE

A	[m^2]	Cross-sectional area
a	[-]	Annular diameter ratio
C	[-]	Correlation coefficient
D	[m]	Diameter
f	[-]	Friction factor
Gr	[-]	Grashof number
L_{dp}	[m]	Pressure drop length
L_{hx}	[-]	Heat exchange length
m	[-]	Correlation exponent
$\dot{m}$	[kg/s]	Mass flow rate
Δp	[Pa]	Pressure drop
Pr	[-]	Prandtl number
Re	[-]	Reynolds number
Re_1	[-]	Lower limit of the transitional flow regime
Re_2	[-]	Upper limit of the transitional flow regime
Ri	[-]	Richardson number
$\bar{V}$	[m]	Average cross-sectional velocity
z	[-]	Correlation exponent for μ_b/μ_{iw}

Special characters

ρ	[kg/m^3]	Density
μ	[kg/ms]	Dynamic viscosity
λ	[-]	Annular geometric parameter
τ	[-]	Wall temperature uniformity

Subscripts

0	Inner wall of outer tube
1	Outer wall of inner tube
iso	Isothermal
in	Inlet
d	Diabatic
h	Hydraulic
iw	Inner tube wall
o	Annular flow passage
out	Outlet

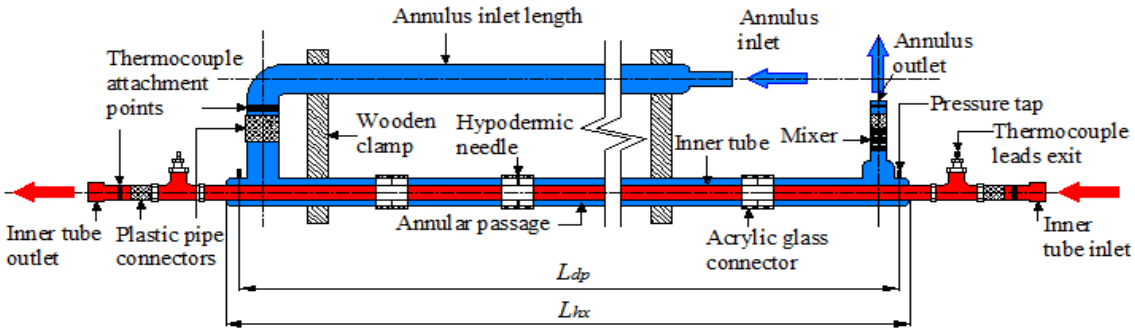

Figure 1: Schematic diagram of a typical tube-in-tube heat exchanger test section (not drawn to scale)

Several researchers have found that the critical Reynolds number is affected by several factors, such as: inlet geometry [6], geometry of conduit [7], thermal boundary condition and convection type [8].

Most research in heat transfer are conducted with either uniform heat flux or uniform wall temperature boundary conditions. Practically, in many tube-in-tube heat exchanger applications the relative flow rates of the heat transfer fluids are such that there is a significant change in temperatures of both of the inner tube and annular fluids. Therefore the wall boundary condition types in this case are non-uniform.

At low Reynolds numbers heat transfer characteristics and fluid flow processes have often been observed to be influenced by buoyancy driven secondary flows. The heat transfer process in this case is referred to as mixed convection. Buoyancy driven secondary flows have been found in several cases to improve heat transfer coefficient [9]. Currently little to no literature exist on the effect of mixed convection on pressure drop in the transitional flow regime of annular passage.

The aim of this paper is to present the impact of varying annular passage dimensions of tube-in-tube heat exchanger have on friction factors in the transitional flow regime. Thermal boundary condition on the inner surface was non-uniform and the flow was associated with buoyancy driven secondary flow. Both the heated and cooled annulus cases were investigated.

EXPERIMENTAL SETUP

The same test facility as is described in some of our previous publications and conference papers [8, 10] was used in this study. The facility consisted of hot water and cold water flow loops. Each loop consisted of a thermostatically controlled water reservoir (either heated or cooled depending on the flow loop), water pumps with accumulators to dampen flow vibration, fluid filters, calibrated Coriolis mass flow meters and suitable hand-operated valves.

Figure 1 shows a schematic representation of a typical test section heat exchanger which was connected to the two flow loops in a counter-flow arrangement. Four test sections (TS1 to TS4), each with different inner tube diameters, D_1 and outer tube diameters, D_0 as presented in Table 1 were investigated.

Table 1: Test section dimensions arranged in descending order of D_h.

Test section	D_1 (mm)	D_0 (mm)	D_h (mm)	a (-)
TS1	12.7	38.88	26.2	0.327
TS2	15.9	38.88	23.0	0.409
TS3	12.7	32.9	20.2	0.386
TS4	15.9	32.9	17.0	0.483

Also shown in the table are hydraulic diameters, $D_h = D_0 - D_1$, annular diameter ratios, $a = D_1/D_0$. The average heat transfer lengths, L_{hx}, and pressure drop lengths, L_{dp}, were 5 070 and 5 050 mm respectively. Each test section was constructed from hard drawn copper tubes, was perfectly horizontal, and had conventional inlet and outlet flow geometries. A calming length was inserted before the inlet port to reduce the impact that upstream disturbances might have on relative pressure drop characteristics. Pressure taps were provided before and after the inlet and outlet annular points. A 2.2 kPa differential pressure transducers which was matched with the prevailing experimental condition in terms of mass flow rate was used to measure the pressure difference. Temperature at different points which were used to determine temperature sensitive properties was measured by T-type thermocouples. Eighteen T-type thermocouples were carefully embedded at 9 axial locations spaced along the length of the inner tube. One thermocouple was fixed at the top and one at the bottom. Sixteen thermocouples were also installed along the outer wall, in sets of two each at 8 locations. Inlet and outlet temperatures of water flowing through the annulus and inner tube were measured at insulated measuring stations. The measuring stations for the annular fluid had eight thermocouples each and those for inner tube fluid had four each. Concentricity between the inner and outer tubes were achieved via carefully inserted hypothermic needles to support the inner tube. All portions of the test section was fully insulated thermally from the lab with 50 mm-thick elastomeric foam sheets with a thermal conductivity of 0.036 W/mK at 23 °C. Inlet temperatures, outlet temperatures, wall temperatures, hot and cold water mass flow

rates and the pressure differences were measured and logged by a National Instruments © data acquisition system operated via a Labview © user-interface.

EXPERIMENTAL PROCEDURE

The pressure transducer was calibrated using a water column and a manometer with accuracy of 0.0055kPa. Thermocouples were calibrated *in situ* using calibrated PT100 probes with absolute accuracies of 0.1°C. Equations were created with which measured data were conditioned during the data-processing stages.

Three different experimental tests series types for each of the four test sections were conducted in terms of the process of the fluid in the annular passage. These were: isothermal adiabatic experiment test series, diabatic cooling test series with hot water in the annulus and cold water in the inner tube, and diabatic heating test series with cold water in the annulus and hot water in the inner tube. Annular mass flow rates were carefully chosen to include all the flow regimes. Isothermal (adiabatic) tests were conducted at an average temperature of 20 °C based on all tests while the diabatic tests were conducted with cold water inlet average temperature of 19 °C and a hot water inlet average temperature of 50 °C based on all tests.

The non-uniform wall temperature boundary was expressed in terms of the degree of the wall temperature uniformity, τ, which was defined as the ratio of the inner wall temperature of the annular passage at the outlet (measured in Kelvin) to that at the inlet (measured in Kelvin), as shown in Equation (1). The τ value was kept at 0.965 for all diabatic tests of this investigation. This was achieved by maintaining the temperature difference between the inlet and outlet on inner tube fluid at approximately 10 °C while varying the annular fluid flow.

$$\tau_{ha} = \overline{T}_{iw,out} / \overline{T}_{iw,in}$$
$$\tau_{ca} = \overline{T}_{iw,in} / \overline{T}_{iw,out} \quad (1)$$

The data points were logged upon reaching a steady state condition when the average annular fluid temperature at the outlet changed within ±0.1°C over a period of one minute. During this period all other temperature readings, as well as the mass flow rates for both inner tube and annulus remained constant. Up to 120 data points were collected for each test data point at 10 Hz.

PROCESSING OF RESULTS

The average friction factors at different Reynolds numbers were determined from the measured pressure drops, Δp, over the pressure drop length, L_{pd}, between the two pressure taps, as:

$$f = \frac{2D_h \Delta p}{\rho_o L_{pd} \overline{V}_o^2} \quad (2)$$

The velocity of the water in the annulus, Equation (3), was determined from the measured mass flow rate in the annulus, and the cross sectional annulus area, and average fluid density. The fluid density was obtained from the method of Popiel and Wojtkowiak [11] at the fluid temperature of annular stream.

$$\overline{V}_o = \dot{m}_o / (\rho_o A_o) \quad (3)$$

The Reynolds number for annular fluid was defined as:

$$\mathrm{Re}_o = \frac{\dot{m} D_h}{\mu_o A_o} \quad (4)$$

An uncertainty analysis of the overall experimental procedures, focusing on the annular side, based on the method of Moffat [12] was performed. All uncertainties were calculated within the 95% confidence interval. Table 2 gives the uncertainties of measuring instruments with their respective range, bias and precision.

It was found that the highest friction factor was 5.5 % at the lower Reynolds number limit of the transitional flow regime for TS4, while the lowest uncertainty was 1.0% at the upper Reynolds number limit of the transitional flow regime for TS1. The highest uncertainties of the friction factors occurred at low Reynolds numbers due to higher uncertainties associated with the differential pressure transducer at lower flow rates.

COMPARISON OF REDUCED DATA WITH LITERATURE

Due to a lack of literature in the transitional flow regime, validation of the test method could only be performed in the turbulent regime as shown in Figure 2. For this purpose a correlation by Filonenko [13] as modified for application to annular flow by Gnielinski [3], Equation (5), was used to validate the friction factors.

$$f_o = \left(1.8 \log_{10} \mathrm{Re}^* - 1.5\right)^{-2} \quad (5)$$

where $$\mathrm{Re}^* = \mathrm{Re}_o \frac{\left(1+a^2\right)\ln a + (1-a^2)}{(1-a)^2 \ln a} \quad (6)$$

Table 2: Applicable experimental measuring ranges and associated uncertainties.

	Range	Uncertainty
T-type thermocouples	-200–350 °C	±0.106 °C
Flow meters	0–0.604 kg/s	±0.1%
	0.3–1.4 kg/s	±0.1%
Differential pressure transducer	0–2.2 kPa	±0.0055 kPa

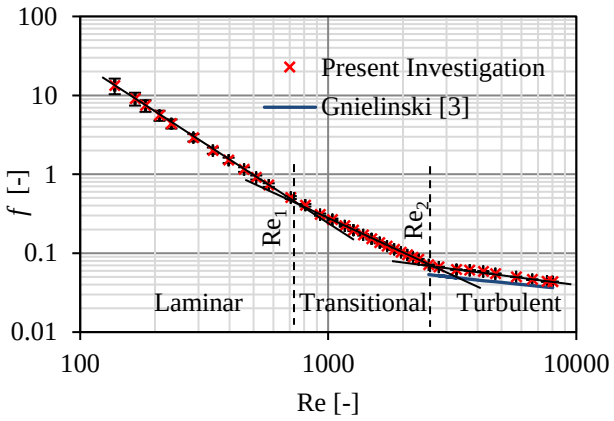

Figure 2: Comparison of friction factor results with a well-known correlation.

The data presented in the figure is for the isothermal test set of TS 2. The figure displays data for the laminar, transitional and turbulent flow regimes. The traced out linear lines segments are described in more detail in next section. From the figure it is observed that the experimentally obtained mean friction factors were higher than those predicted by Equation (5). This is due to the influence of the hydrodynamic entrance region when the flow is developing. In the hydrodynamic entrance region, the wall shear stress is highest at the pipe inlet where the boundary layer thickness is the smallest, and decreases along the flow direction. Therefore, the pressure drop is the highest in the entrance region of a pipe. Hence, it always increases the mean friction factor for the whole pipe. Equation (5) under-predicted the mean experimental friction factors by 10%, 12%, 18% and 23% for test sections TS 1, TS 2, TS 3 and TS 4 respectively.

RESULTS AND DISCUSSIONS

Firstly, the lower and upper limits of the transitional flow regimes for the different test sections were identified by analysing test data that encompassed all flow regimes. For this purpose, the lengthwise averaged friction factors were plotted against the Reynolds number (both on a logarithmic scale) for all the test cases and carefully analysed to identify changes in the characteristic gradients of the plots. By inspection it was observed that the trends of the graph are well-described by linear line segments with different gradients for laminar, transitional and turbulent regime ranges. Figure 2 shows how the straight lines that were generated using root mean square deviation method were used to trace out the regimes. Line intercepts Re_1 and Re_2 indicated the lower and upper Reynolds number limits of the transitional flow regimes limits of the flow regime regions, while the low and high Reynolds number ranges indicate the laminar and turbulent regimes, respectively. Figure 3 shows Reynolds number transitional regime spans for all the test sections for isothermal, heated and cooled cases.

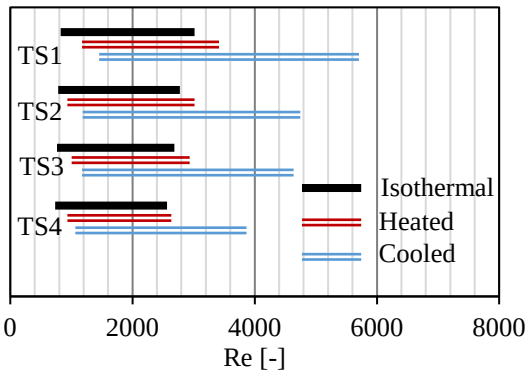

Figure 3: Reynolds number transitional regime spans.

Buoyancy-driven secondary flow

In order to better interpret the observed Re_1 and Re_2 trends, as well as the results that will follow, the impact of the convection types (natural, mixed and forced), as indicated by the Richardson number, must be considered. The boundaries between the different convection types are determined by the Richardson number, $Ri = Gr/Re^2$. Mixed convection conditions are considered when $0.1 \leq Ri \leq 10$. For $Ri > 10$, the flow is treated as natural convection, and the forced convection is considered when $Ri < 0.1$.

It was found that, for all the test sections (for both heated and cooled annuli), laminar flow cases exhibited mixed convection, while the turbulent flow cases exhibited forced convection. In most of the tests, the indicative cut-off point ($Ri \approx 0.1$) between the mixed and forced convection was found to fall within the transitional flow regimes. Figure 4 depicts the spread of experimental data in the mixed convection regime. The mixed convection is more prevalent for the test section with larger hydraulic diameters. As the hydraulic diameter decreases, the Ri values and mixed convection portion of the transitional flow regime decrease as well. Compared between the heated and cooled annulus cases, the cooled cases are more likely to have mixed convection conditions.

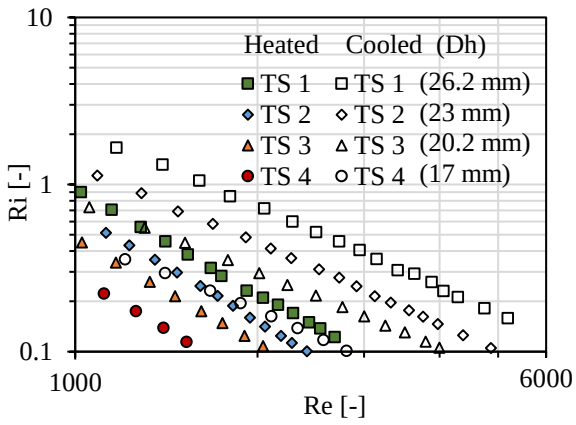

Figure 4: Richardson numbers for heated and cooled annulus cases.

In all the cases considered as observed in Figure 3, the Re_1 values were higher for TS 1, followed by TS 2, TS 3 and TS 4 consecutively. This trend relates linearly to the hydraulic diameters of these test sections. Similarly, Re_2 was also higher for the test section with larger hydraulic diameters. The Reynolds number spans of the transitional flow regimes ($Re_2 - Re_1$) were also found to be related to the hydraulic diameters. Larger hydraulic diameters exhibited longer spans and smaller hydraulic diameters exhibited shorter spans.

It was also observed that the Re_1 value based on the friction factor was lowest for the isothermal cases, followed by the heated cases, and finally the cooled cases, which exhibited the largest Re_1 values. The $Re_2 - Re_1$ ranges for the cooled cases were the longest, followed by the heated cases. For the isothermal cases, these ranges were the shortest.

The differences in the Re_1 and Re_2 values obtained from the different test sections for isothermal cases could be due to changes in the annular dimensions. In the diabatic cases, apart from the annular dimensions, changes in the friction factors in the transitional flow regime could also be due to temperature variation differences between the annular fluid and the inner wall of the annular passage, as well as the fluid viscosity, which is relatively temperature sensitive.

Mean friction factor

Figure 5 presents the friction factors of the different test sections for a) isothermal conditions [14] and b) diabatic conditions. It can be seen that the friction factors of TS 1 were highest, followed by TS 2, TS 3 and TS 4 for all the cases (isothermal, heated and cooled). Therefore, the friction factors were found to be significantly dependent on geometric parameters of the tests sections. For any particular Reynolds number value, higher friction factors were present for larger annular gap sizes.

The friction factors for the cooled cases were higher than for the heated cases in all the test sections and those for isothermal case were the lowest. The difference in friction factors between the isothermal and diabatic cases, and also between the cooled and heated annulus cases for a particular test section, could be due to various factors, including the different viscosity values on the inner wall of the annulus, as determined by wall temperature.

Correlation

Based on the datasets, it was found via inspection that a plausible combined effect of the annular diameter ratio, hydraulic diameter and heat transfer and pressure drop length on the friction factors could be described in dimensionless form as:

$$\lambda = aL_{dp}/D_h \tag{6}$$

Firstly, the isothermal friction factors, f_{iso}. For the four test section were correlated as:

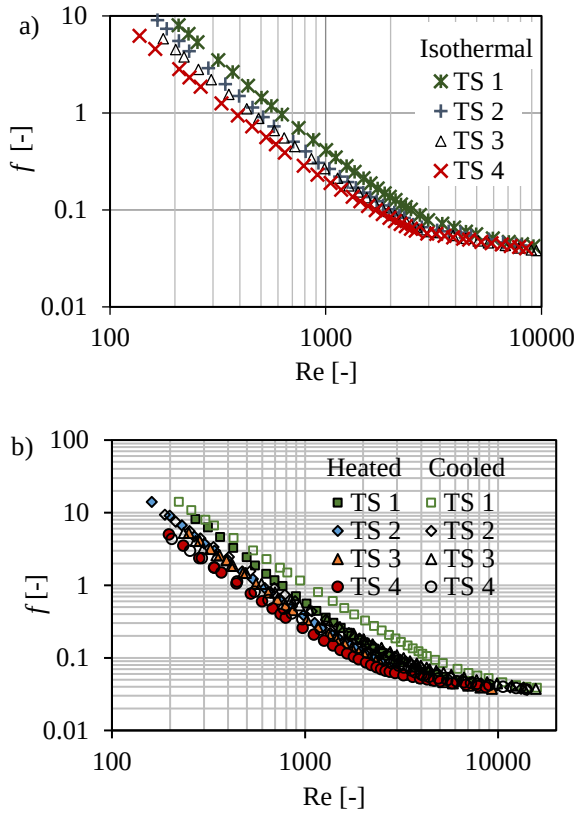

Figure 5: Friction factors for different test sections' values: (a) for isothermal case; and (b) for heated and cooled annulus cases.

$$f_{iso} = C_{iso}(\lambda)\mathrm{Re}^{-m(\lambda)} \tag{7}$$

Where C_{iso} and exponent m are given by:

$$C_{iso} = 2.784\lambda^2 - 717.574\lambda + 46425.43 \tag{8}$$

$$m = -0.00357\lambda + 1.721\,. \tag{9}$$

These and the other coefficient and exponent expressions in this paper were obtained from equations generated through line fit that best described the relationships between friction factors and the relevant parameters.

Diabatic friction factors, f_d, were adjusted from the isothermal friction factors by incorporating the viscosity ratio between the bulk fluid state and the fluid state at the heat transfer wall:

$$f_d = f_{iso}\lambda^z C_d(\mu_b/\mu_{iw}) \tag{10}$$

Coefficient C_d and exponent z are dependent on Grashof and Prandtl numbers [6].

Expressions for the coefficient and exponent in Equation (10) for the heated and cooled annulus cases were obtained as:

For heated annuli:

$$C_d = 37\times10^{3}\left(\mathrm{Gr}^{0.01}\,\mathrm{Pr}^{2.9}\right)^{-1.74} \quad (11)$$

$$z = 1.3\times10^{-3}\left(\mathrm{Gr}^{0.01}\,\mathrm{Pr}^{2.9}\right) - 0.50 \quad (12)$$

For an applicable range of $1\,400 \le \mathrm{Re} \le 2\,500$, $187 \le \mathrm{Gr}^{0.01}\,\mathrm{Pr}^{2.9} \le 244$, $1.36 \le \mu_b/\mu_{iw} \le 1.46$ and $64 \le \lambda \le 144$.

For cooled annuli:

$$C_d = 0.86\left(\mathrm{Gr}^{0.01}\,\mathrm{Pr}^{2.9}\right)^{0.37} \quad (30)$$

$$z = -0.48\times10^{3}\left(\mathrm{Gr}^{0.01}\,\mathrm{Pr}^{2.9}\right) - 0.66 \quad (31)$$

For an applicable range of $1\,400 \le \mathrm{Re} \le 2\,500$, $60 \le \mathrm{Gr}^{0.01}\,\mathrm{Pr}^{2.9} \le 75$, $0.73 \le \mu_b/\mu_{iw} \le 0.77$ and $64 \le \lambda \le 144$.

Figure 6 shows the comparison between the experimental and predicted friction factors for the heated and cooled annulus cases. The agreement between the experimental results and the proposed correlations was good, with all the data points within a ±11% error band.

CONCLUSION

This study provided the characteristics of the isothermal and diabatic pressure drop (friction factor) in the transitional flow regime associated with mixed convection in developing flow. Thermal boundary condition on the inner surface was non-uniform. It was found that the dimensions of annular passage had impact on friction factor in the transitional flow regime. It was also found that the range of the transitional flow regime is dependent on the geometric parameters of the annulus. A new non dimensional annular passage parameter based on the annular diameter ratio, hydraulic diameter and heat transfer and pressure drop length is proposed to correlate the experimental data. New correlations were developed for the prediction of isothermal and diabatic (cooled and heated cases) friction factors in the transition flow regime of annular passage.

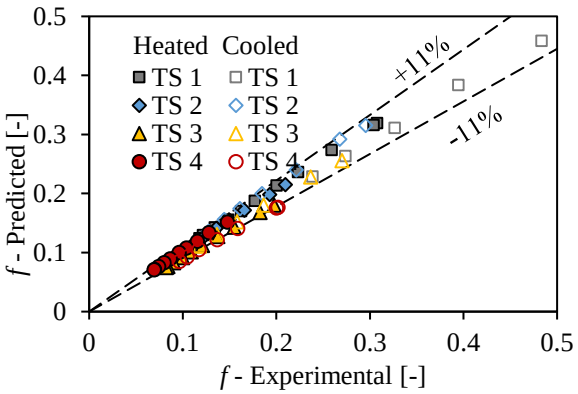

Figure 6: Comparison between experimental and predicted friction factor results.

REFERENCES

[1] Çengel Y.A., and Ghajar A.J., Heat and mass transfer, 2011, New York, Mc Graw Hill.

[2] Meyer J.P., Heat transfer in tubes in the transitional flow regime, *Proceedings of the 15th International Heat Transfer Conference*, 2014, Kyoto, Japan

[3] Gnielinski V., Berechnung des druckverlustes in glatten konzentrischen ringspalten bei ausgebildeter laminarer und turbulenter strömung, *Chem. Ing. Techn.*, Vol. 79, 2007, pp. 91 - 95

[4] Van Zyl W.R., Dirker J., and Meyer J.P., Single-phase convective heat transfer and pressure drop coefficients in concentric annuli, *Heat Transfer Engineering*, Vol. 34, No. 13, pp. 1112 – 1123

[5] Prinsloo F.P.A., Dirker J., and Meyer J.P., Heat transfer and pressure drop characteristics in the annuli of tube-in-tube heat exchangers (Horizontal lay-out), *Proceedings of the 15th International Heat Transfer Conference*, Kyoto, Japan, Paper number 9225, August 2014

[6] Tam L., and Ghajar A.J., Effects of inlet geometry and heating on the fully developed friction factor in the transition region of a horizontal tube. *Experimental Thermal and Fluid Science*, Vol. 15, 1997, pp. 52 – 64

[7] Lu G., and Wang J., Experimental investigation on heat transfer characteristics of water flow in a narrow annulus, *Applied Thermal Engineering*, Vol. 28, 2008, pp. 8 – 13

[8] Ndenguma D.D., Dirker J., and Meyer J.P., Transitional flow regime heat transfer and pressure drop in an annulus with non-uniform wall temperatures, *International Journal of Heat and Mass Transfer*, Vol. 108, 2017, pp 2239 – 2252

[9] Kakaç S., Shah R.K., and Aung W., Handbook of single-phase convective heat transfer, 1987, New York, Interscience

[10] Ndenguma D.D., Dirker J., and Meyer J.P., Transitional flow regime heat transfer in annular passage associated with mixed convection and non-uniform wall temperature boundary condition, *Proceedings of the 12th Heat Transfer, Fluid Mechanics and Thermodynamics Conference*, Costa del Sol, Spain, Paper number 1570248845, July 2016

[11] Popiel C.O., and Wojtkowiak J., Simple formulas for thermophysical properties of liquid water for heat transfer calculations (from 0°C to 150°C), *Heat Transfer Engineering*, Vol. 19, 1998, pp. 87 – 101

[12] Moffat R.J., Describing the uncertainty in experimental results, *Experimental Thermal Fluid Science*, Vol. 105, 1983, pp 498 – 504

[13] Filonenko G.K., Hydraulic resistance of pipes, *Teploenergetika*, Vol. 1, No. 4, 1954, pp. 40 – 44

[12] Moffat R.J., Describing the uncertainty in experimental results, *Experimental Thermal Fluid Science*, Vol. 105, 1983, pp 498 – 504

[13] Filonenko G.K., Hydraulic resistance of pipes, *Teploenergetika*, Vol. 1, No. 4, 1954, pp. 40 – 44

[12] Moffat R.J., Describing the uncertainty in experimental results, *Experimental Thermal Fluid Science*, Vol. 105, 1983, pp 498 – 504

[13] Filonenko G.K., Hydraulic resistance of pipes, *Teploenergetika*, Vol. 1, No. 4, 1954, pp. 40 – 4

[14] Ndenguma D.D., Dirker J., and Meyer J.P., Heat transfer and pressure drop in annuli with approximately uniform internal walll temperatures in the transitional flow regime, *International Journal of Heat and Mass Transfer*, Vol. 111, 2017, pp 429 – 441